

University of Groningen

Magnetic versus structural properties of Co nanocluster thin films

Koch, S. A.; te Velde, R. H.; Palasantzas, G.; de Hosson, J. Th. M.

Published in:
Applied Physics Letters

DOI:
[10.1063/1.1641511](https://doi.org/10.1063/1.1641511)

IMPORTANT NOTE: You are advised to consult the publisher's version (publisher's PDF) if you wish to cite from it. Please check the document version below.

Document Version
Publisher's PDF, also known as Version of record

Publication date:
2004

[Link to publication in University of Groningen/UMCG research database](#)

Citation for published version (APA):

Koch, S. A., te Velde, R. H., Palasantzas, G., & de Hosson, J. T. M. (2004). Magnetic versus structural properties of Co nanocluster thin films: A magnetic force microscopy study. *Applied Physics Letters*, 84(4), 556-558. <https://doi.org/10.1063/1.1641511>

Copyright

Other than for strictly personal use, it is not permitted to download or to forward/distribute the text or part of it without the consent of the author(s) and/or copyright holder(s), unless the work is under an open content license (like Creative Commons).

Take-down policy

If you believe that this document breaches copyright please contact us providing details, and we will remove access to the work immediately and investigate your claim.

Downloaded from the University of Groningen/UMCG research database (Pure): <http://www.rug.nl/research/portal>. For technical reasons the number of authors shown on this cover page is limited to 10 maximum.

Magnetic versus structural properties of Co nanocluster thin films: A magnetic force microscopy study

S. A. Koch, R. H. te Velde, G. Palasantzas, and J. Th. M. De Hosson^{a)}

Department of Applied Physics, Materials Science Centre and the Netherlands Institute for Metals Research, University of Groningen, Nijenborgh 4, 9747 AG Groningen, The Netherlands

(Received 6 August 2003; accepted 21 November 2003)

Magnetic force microscopy (MFM) has been employed to study thin films consisting of low-energy-deposited cobalt nanoclusters. On continuous cluster layers a clear magnetic stray field pattern can be observed, although measurements on individual clusters are complicated by interference from topography. The magnetic correlation length determined from MFM images is substantially larger than the size of a single cluster. This indicates that the clusters are magnetically coupled to form stable domains associated with the formation of a correlated super-spin-glass state. © 2004 American Institute of Physics. [DOI: 10.1063/1.1641511]

Nanostructured ferromagnets are expected to form an important class of materials in future technologies.^{1,2} The properties of isolated magnetic particles/grains change remarkably as their size D is reduced to fall within the nanometer range. In fact, particles smaller than the width of a domain wall (~ 50 nm) are always in a single-domain state, with the magnetization aligned with the anisotropy axis.^{1,2} Above the onset of superparamagnetism (typically $D > 10$ nm)² these particles have a large coercivity. For applications in magnetic storage media, high anisotropy, and low coupling between the grains are the requirements to maintain the independence of individual memory units.³

In contrast, if isolated grains aggregate to form densely packed nanostructured magnets, the exchange coupling between the randomly oriented grains largely determines the magnetic behavior.¹ As a result, these materials are often magnetically soft allowing the integration of transformers and inductors into silicon integrated circuitry. Soft-magnetic films are also widely used in modern electromagnetic devices as high-frequency (> 100 MHz) field-amplifying components, for example in read-write heads for computer disk memories, and as a magnetic shielding material, for example in tuners. To obtain the desired properties (low coercivity, little strain, and very small magnetostriction), the use of materials with grain size on the order of 10 nm, such as nanocrystalline cobalt, becomes attractive.⁴ The coercivity in such materials can be tuned by variation of the grain size, where a distinct maximum at grain sizes of typically some tens of nanometers was revealed followed by a sharp fall-off for smaller grains.⁵

Therefore, in order to design magnetic materials for specific applications, it is important to understand the intricate relationship between magnetic properties and nanoscale-structured structural features (i.e., related to film morphology). For this reason, efforts are in progress to image the domain structure for these materials and to reveal their magnetic dynamics. In Fe and Ni with grain sizes ~ 10 – 100 nm, the magnetic correlations were found to extend over many grains.¹ In hcp Co, the observed correlation lengths were on

the order of the grain size due to stronger magnetocrystalline anisotropy.¹ For both Ni and Co porous films consisting of low-energy-deposited fcc clusters with a diameter of 3–4 nm, local magnetic order of the extent of a grain was observed.⁶ In *in situ* electrical resistivity and magnetization studies of deposited Co clusters with 6–13 nm diameter, a transition from superparamagnetic to ferromagnetic behavior was observed as a function of coverage, even prior to the percolation threshold,⁷ suggesting that long-range dipole interactions between superparamagnetic clusters can exist (depending on coverage).

Unlike for Co granular magnetic recording media,⁸ so far there have not been any magnetic force microscopy (MFM)^{8,9} observations of magnetic stray field patterns from Co nanocluster-assembled films. This will be the topic of our study, focusing on the determination of *magnetic* and *spatial* correlation lengths. MFM can provide information about the local magnetic structure that is not accessible via other methods (e.g., superconducting quantum interference device methods).^{8,9} However, a precise comparison between height and phase images is required to separate true magnetic information from possible interference caused by the surface topography. For this purpose, nonmagnetic Nb nanocluster films were also analyzed.

Clusters of either Co or Nb were produced with the Oxford Applied Research NC200U nanocluster deposition source that is equipped with a dc magnetron.¹⁰ Atoms from the metal target were sputtered into a water-cooled condensation region containing Ar at a pressure of $(2\text{--}5) \times 10^{-3}$ mbar (base pressure 2×10^{-8} mbar). The substrates, Si(100) with the native oxide, were held at room temperature. The mean cluster size is ~ 8 nm with a small standard deviation $\sim 10\%$, even without mass selection of the free clusters. During the deposition process random stacking of clusters leads to the formation of a porous film,¹¹ with clusters remaining largely intact due to their low impact energy.

The Co and Nb films were sputter-coated with 2 nm of Pd to reduce sticking of clusters to the MFM probe tip. Imaging was performed with the Dimension 3100 atomic force microscope (AFM) (Digital Instruments) operating in tapping/lift mode, which combines constant interaction and

^{a)}Electronic mail: hossonj@phys.rug.nl

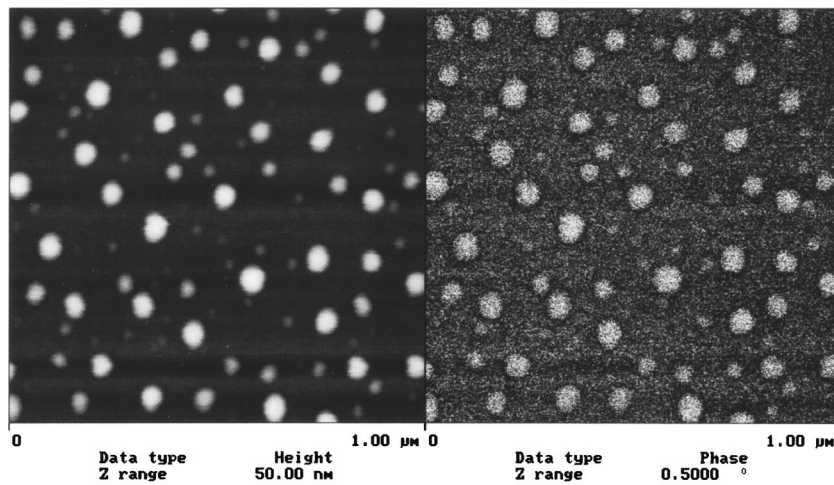


FIG. 1. Topography AFM image (left) of an open film of Nb nanoclusters on a Si substrate ($1 \times 1 \mu\text{m}^2$ area), and the corresponding phase change MFM image (right).

constant height modes in order to separate topographic and magnetic signals.^{12,13} The tips were of the commercially available Si-type¹⁴ with a 50 nm coating of CoCr alloy. They were magnetized in the z direction parallel to the tip axis. In addition, external magnetic fields were applied to a Co film in both out-of-plane (\perp) and in-plane (\parallel) directions to observe the effect on the remanent state.

Figure 1 shows an open Nb nanocluster film. The MFM image on the right demonstrates a positive phase shift at each cluster position of magnitude up to 0.3° , which would indicate a repulsive interaction. The phase intensity seems to be directly related to the cluster height, while the apparent cluster diameter (within the range from 40 to 60 nm) is identical in both images. MFM measurements on deposited magnetic Co clusters yielded comparable results. Therefore, the phase shifts were not caused by any magnetic interaction. Electrostatic forces could also be ruled out by scanning with a non-magnetized tip; this made no difference either on Co or Nb clusters. Very slow scanning (scan rate 0.25 Hz) only reduced the noise while the phase shifts at the clusters remained unchanged.¹⁴ Notably, the observed phase shift is always positive, while superparamagnetic and van der Waals interactions would lead to a negative contrast.¹⁵ Moreover, van der Waals forces only become significant for tip-sample distances < 10 nm,⁸ which is below the values used here. The MFM measurements on single particles suffer from the topographic contamination of magnetic field data^{15–17} which

can be alleviated by using large enough lift heights (> 17 nm; tip-sample distance = lift height + oscillating amplitude). The topographic interference is possibly caused by air damping of the cantilever oscillation.¹⁴

Figure 2 shows a closed Co film of thickness of 375 nm, and the corresponding MFM recorded with a lift height of 40 nm. Cluster contours are still resolved due to the topography effect just described, but here the main signal arises from magnetic interactions. Regions are observed where the intensity is either bright (repulsive interaction) or dark (attractive interaction). The rms value of the phase shift over the entire image is 0.20° . Films with lower thickness (down to ~ 75 nm) gave similar results. The magnetic domains have irregular shapes and they extend over numerous clusters, with edges corresponding to cluster edges. In order to quantify the difference in local order between topography and MFM, an attempt was made to calculate the correlation lengths for both types of data on $8 \mu\text{m}$ scan size images.

The height data exhibit self-affine scaling, where the height-height correlation function $g(x) = \langle [h(x) - h(0)]^2 \rangle$ is proportional to a power of x at small lengths $x (< \xi)$ with ξ the in-plane roughness correlation length). For $x \gg \xi$, $g(x)$ saturates to the value $2w^2$ with $w = \{\langle h^2 \rangle\}^{1/2}$ the rms roughness amplitude. The correlation length of $\xi = 91$ nm was found from the intersection of power-law and saturation lines, which is close to the knee regime in a log-log plot [Fig. 3(a)]. On the other hand, since the phase data do not

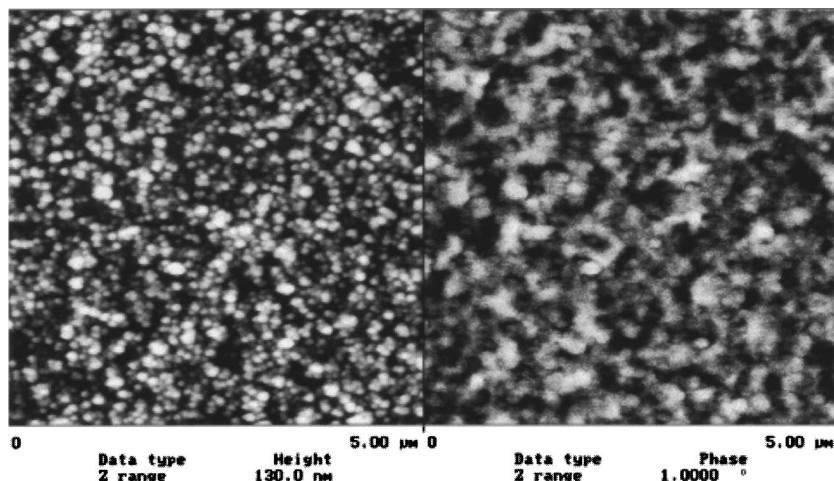


FIG. 2. Height (left) and phase (right) images of a 375-nm-thick dense Co nanocluster film (scan size $5 \mu\text{m}$).

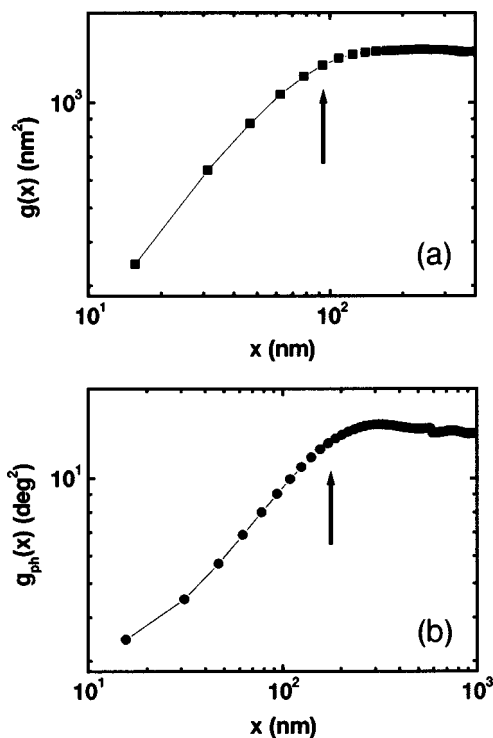


FIG. 3. Height–height (a) and phase change (b) correlation data for the films shown in Fig. 2 for scan size $8\ \mu\text{m}$.

follow power-law behavior, the correlation length ($\xi_{\text{ph}} \approx 200\ \text{nm}$) was estimated directly from the knee regime of $g_{\text{ph}}(x)$ as can be seen in Fig. 3(b).

Within the random anisotropy model,^{1,18} when the random field $H_r (= 2K_r/M_s)$, with K_r the randomly oriented grain anisotropy and M_s the saturation magnetization) is larger than the exchange field $H_{\text{ex}} (= 2A/M_s R_{\text{cor}}$, with A the exchange constant due to grain–grain interaction and R_{cor} correlation length of the local anisotropy axis), the magnetic vector in each particle points along the local intraparticle anisotropy axis. With increasing interparticle exchange (or decreasing intraparticle anisotropy), the configuration becomes a correlated super-spin glass (CSSG).¹⁸ The CSSG state is clearly observed in the case of our Co nanocluster films with a magnetic correlation length that is twice the geometric correlation length. Therefore, the magnetic structure is not only determined by the deposition of randomly oriented grains, but also by the magnetic coupling between them. Indeed, since we have $\xi_{\text{ph}} = D/\lambda_r$ ($\lambda_r = H_r/H_{\text{ex}}$),¹⁸ we can estimate the ratio of random to exchange fields $\lambda_r = 0.22$ for particle diameter $D = 10\ \text{nm}$ and $\xi_{\text{ph}} = 200\ \text{nm}$.

Next, the 375-nm-thick Co film was exposed to various external magnetic fields, and MFM images of the remanent state were collected. The rms value of the phase shift increases from $0.20^\circ \rightarrow 0.29^\circ$ after the initial exposure to 2.4 kG normal to the plane (Fig. 4). Increasing the field further to 4.1 kG has little effect, indicating saturation. Subsequent application of equally strong fields parallel to the plane leads to a relatively sharp decrease in signal. This can be expected because MFM is sensitive to field components along the z

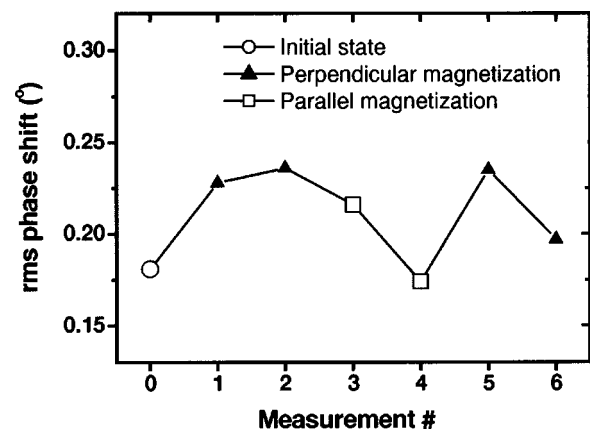


FIG. 4. Rms values of the phase shift calculated over entire MFM images ($8\ \mu\text{m}$ size) after applying magnetic fields of 2.4, 4.1, 7.0, and 11.4 kG (directions indicated).

direction, while the parallel magnetization configuration already produces weaker stray field because of the shape effect (i.e., demagnetizing factor). The remaining two data points in Fig. 4 correspond to higher fields of 7.0 and 11.4 kG in the perpendicular direction, respectively. No changes in the domain distribution and morphology were observed.

We would like to acknowledge useful discussions with Prof. Chris Binns (UL, UK), Dr. M. Donahue (NIST, USA), Dr. M. Raša (UT, NL), and Prof. A. P. Philipse (UT, NL).

- ¹J. F. Löffler, H.-B. Braun, and W. Wagner, *Phys. Rev. Lett.* **85**, 1990 (2000).
- ²*Nanomaterials: Synthesis, Properties and Applications*, edited by A. S. Edelstein and R. C. Cammarata (Institute of Physics, Philadelphia, 1996).
- ³W. Wernsdorfer, E. Bonet Orozco, K. Hasselbach, A. Benoit, B. Barbara, N. Demoncey, A. Loiseau, H. Pascard, and D. Mailly, *Phys. Rev. Lett.* **78**, 1791 (1997); for inelastic neutron scattering, see M. F. Hansen, F. Bødker, S. Mørup, K. Lefmann, K. N. Clausen, and P.-A. Lindgård, *ibid.* **79**, 4910 (1997).
- ⁴Y. Yoshizawa, S. Oguma, and K. Yamauchi, *J. Appl. Phys.* **64**, 6044 (1988).
- ⁵G. Herzer, *J. Magn. Magn. Mater.* **112**, 258 (1992).
- ⁶J. Tuaillon, V. Dupuis, P. Mélinon, B. Prével, M. Treilleux, A. Perez, M. Pellarin, J. L. Vialle, and M. Broyer, *Philos. Mag. A* **76**, 493 (1997).
- ⁷S. Yamamuro, K. Sumiyama, T. Kamiyama, and K. Suzuki, *J. Appl. Phys.* **86**, 5726 (1999).
- ⁸S. Porthun, L. Abelmann, and C. Lodder, *J. Magn. Magn. Mater.* **182**, 238 (1998).
- ⁹U. Hartmann, *Annu. Rev. Mater. Sci.* **29**, 53 (1999).
- ¹⁰<http://www.oaresearch.co.uk/cluster.htm>. See also H. Haberland, M. Moseler, Y. Qiang, O. Rattunde, T. Reiners, and Y. Thurner, *Surf. Rev. Lett.* **3**, 887 (1996).
- ¹¹G. Palasantzas, S. A. Koch, and J. Th. M. De Hosson (unpublished).
- ¹²P. Grutter, H. J. Mamin, and D. Ruger, *Scanning Tunneling Microscopy II*, edited by R. Wiesendanger and H. J. Guntherodt (Springer, Berlin, 1992), p. 151.
- ¹³S. Porthun, L. Abelmann, and C. Lodder, *J. Magn. Magn. Mater.* **182**, 238 (1998).
- ¹⁴<http://www.veeco.com/>
- ¹⁵M. Raša, B. W. M. Kuipers, and A. P. Philipse, *J. Colloid Interface Sci.* **250**, 303 (2002).
- ¹⁶C. E. Vallet, C. W. White, S. P. Withrow, J. D. Budai, L. A. Boatner, K. D. Sorge, J. R. Thompson, K. S. Beaty, and A. Meldrum, *J. Appl. Phys.* **92**, 6200 (2002).
- ¹⁷M. Miyasaka, Y. Saito, and H. Nishide, *Adv. Funct. Mater.* **13**, 113 (2003).
- ¹⁸C. Binns, M. J. Maher, Q. A. Pankhurst, D. Kechrakos, and K. N. Trohidou, *Phys. Rev. B* **66**, 184413 (2002).